

BCL6 programs lymphoma cells for survival and differentiation through distinct biochemical mechanisms

Samir Parekh,¹ Jose M. Polo,¹ Rita Shaknovich,² Przemyslaw Juszczynski,³ Paola Lev,¹ Stella M. Ranuncolo,¹ Yingnan Yin,¹ Ulf Klein,⁴ Giorgio Cattoretti,⁵ Riccardo Dalla Favera,⁴ Margaret A. Shipp,³ and Ari Melnick¹

¹Department of Developmental and Molecular Biology; ²Department of Pathology, Albert Einstein College of Medicine, Bronx, NY; ³Department of Medical Oncology, Dana Farber Cancer Institute, Boston, MA; ⁴Institute for Cancer Genetics, Columbia University, New York, NY; ⁵Department of Pathology, Università degli Studi di Milano-Bicocca, Monza, Italy

The BCL6 transcriptional repressor is the most commonly involved oncogene in diffuse large B-cell lymphomas (DLBCLs). Constitutive expression of BCL6 mediates lymphomagenesis through aberrant proliferation, survival, and differentiation blockade. Binding of BCL6 to the SMRT/N-CoR corepressors mediates the BCL6 survival effect in DLBCL. Although the basis for differentiation blockade is unknown in DLBCL, recent data suggest that BCL6 binding to the MTA3 corepressor might be involved. We report that BCL6 and MTA3 are coexpressed in nor-

mal germinal center B cells and DLBCL. Depletion of MTA3 in DLBCL cells induced a differentiation-related BCL6 target gene (PRDM1), but not target genes involved in survival. Accordingly, MTA3 and PRDM1 expression are mutually exclusive in germinal center B cells. We performed chromatin immunoprecipitation (ChIP)-on-chip mapping of the PRDM1 locus, identifying a novel BCL6 binding site on intron 3 of the PRDM1 gene, and show that BCL6 recruits MTA3 to this site. In DLBCL cells, MTA3 depletion induced plasmacytic differentiation

but did not decrease viability of DLBCL cells. However, MTA3 depletion synergized with a specific BCL6 inhibitor that blocks SMRT/N-CoR binding to decrease DLBCL viability. Taken together, these results show that BCL6 regulates distinct transcriptional programs through the SMRT/N-CoR and MTA3 corepressors, respectively, and provides a basis for combinatorial therapeutic targeting of BCL6. (Blood. 2007;110:2067-2074)

© 2007 by The American Society of Hematology

Introduction

The BCL6 (B-cell lymphoma-6) transcriptional repressor is tightly linked to the pathogenesis of diffuse large B-cell lymphomas (DLBCLs). BCL6 is often constitutively expressed in DLBCL due to promoter translocations or point mutations of negative regulatory elements.^{1,2} In normal B-cell development, BCL6 is required for formation of germinal centers (GCs), from which many B-cell lymphomas are apparently derived. In GCs, B cells proliferate rapidly while undergoing immunoglobulin (Ig) affinity maturation through class-switch recombination and somatic hypermutation.^{3,4} BCL6 facilitates Ig affinity maturation by repressing target genes involved in DNA damage responses, cell cycle, and other processes (such as *ATR*, *TP53*, and *CDKN1A*).⁵⁻⁸ BCL6 can also block the further differentiation of GC B cells, in part by directly or indirectly repressing the *PRDM1* (Pr domain-containing protein 1) master regulator of plasma cell differentiation.⁹⁻¹² Both of these effects might be important in imposing the phenotype of DLBCL.

BCL6 represses its target genes by recruiting corepressor proteins through its 3 different protein domains. Among these, the N-terminal BTB/POZ (bric a brac, tramtrack, broad complex) domain binds to SMRT (silencing mediator for retinoid and thyroid receptor), N-CoR (nuclear hormone receptor corepressor), and BCoR (BCL6 corepressor).^{13,14} BCL6 specifically recruits SMRT/N-CoR/BCoR through a lateral groove motif that is formed upon dimerization of its BTB domain.¹⁵ Blockade of the BCL6 lateral

groove by a specific peptide inhibitor (BPI, BCL6 peptide inhibitor) derepressed certain BCL6 target genes, blocked proliferation and survival of human DLBCL cells, and abrogated GC formation in mice.¹⁶ However, BPI did not induce *PRDM1* expression or further differentiation of DLBCL cells, suggesting that these effects might be mediated through an alternative mechanism.

BCL6 also recruits the NuRD (nucleosome remodeling and deacetylase) complex by directly binding to its MTA3 (metastasis-associated 3) subunit.¹⁷ The interaction involves the middle region of BCL6 (or RD2 [repression domain 2]) and the C-terminal region of MTA3. MTA3 depletion from Burkitt lymphoma cells induced the expression of plasmacytic features and forced expression of MTA3 and BCL6 in myeloma cells caused cells to at least partial reversion to a GC/mature B cell phenotype.¹⁷ Among genes repressed (directly or indirectly) by MTA3 was *PRDM1*. Taking together these 2 lines of evidence, we hypothesized that BCL6 mediates DLBCL survival and differentiation through distinct biochemical mechanisms: the former through BTB domain recruitment of SMRT/N-CoR/BCoR, and the latter through RD2 recruitment of MTA3.

Herein, we examine define the expression pattern of BCL6 and MTA3 in normal human lymph nodes and primary DLBCLs and show that BCL6 and MTA3 are coexpressed in normal GC B cells (GCB) and DLBCLs of the GCB- and the BCL6-dependent B-cell

Submitted January 30, 2007; accepted May 28, 2007. Prepublished online as *Blood* First Edition paper, June 1, 2007; DOI 10.1182/blood-2007-01-069575.

An Inside *Blood* analysis of this article appears at the front of this issue.

The online version of the article contains a data supplement.

The publication costs of this article were defrayed in part by page charge payment. Therefore, and solely to indicate this fact, this article is hereby marked "advertisement" in accordance with 18 USC section 1734.

© 2007 by The American Society of Hematology

receptor (BCR) subtypes. In BCL6-dependent DLBCL cell lines, depletion of MTA3 induced PRDM1 expression and phenotypic changes typical of plasma cell differentiation, but had no effect on survival. BCL6 recruited MTA3 to a site that we mapped to intron 3 of *PRDM1* by genomic tiling chromatin immunoprecipitation (ChIP) on chip. The combination of lateral groove inhibition and MTA3 depletion resulted in greater killing of lymphoma cells, suggesting that combinatorial targeting of the BCL6 transcriptional program might have greater antilymphoma therapeutic effects. These results demonstrate that BCL6 mediates its biological effects through 2 distinct and separate biochemical mechanisms.

Materials and methods

Cell lines and cell culture

Ramos, Pfeiffer, SUDHL4, and Toledo cells were grown in RPMI 1640 media containing 2 mM L-glutamine and 10% fetal bovine serum (FBS; Gemini Bio-Products, Woodland, CA). LY1, LY4, and LY7 cells were grown in Iscove medium supplemented with 10% FBS.

Cell lysis and Western blot

Cells were lysed in RIPA buffer containing 50 mM Tris-HCl (pH 7.4), 150 mM NaCl, 1 mM PMSF, 1 mM EDTA, 10% NP-40, 1% sodium deoxycholate, and 0.1% SDS. Protein extracts were resolved by SDS-PAGE followed by immunoblotting with BCL6 antibody (N-3 antibody, Santa Cruz Biotechnologies, Santa Cruz, CA), MTA3 (EMD Biosciences, San Diego, CA), PRDM1 (Abcam, Cambridge, MA), and actin antibody (AC15; Sigma, St Louis, MO), and detection by electrochemiluminescence (ECL; Santa Cruz Biotechnology).

Isolation of primary B-cell populations

Routine human tonsillectomy specimens were obtained from the Montefiore Children's Hospital with approval of the Albert Einstein College of Medicine and Montefiore Hospital Institutional Review Boards and in accordance with the Helsinki protocols. After mincing, tonsillar mononuclear cells were isolated by HISTOPAQUE-1077 (Sigma) density centrifugation. Naive B cells (NBCs), centroblasts (CBs), and centrocytes (CCs) were separated by magnetic cell separation using the MidiMACS system (Miltenyi Biotec, Auburn, CA) following published protocols.¹⁸ The purity of the isolated B-cell populations was determined by FACScan (Becton Dickinson, Franklin Lake, NJ) analysis. NBCs were IgD⁺, CD38^{low}, and CD27⁻; CBs were CD77⁺ and CD38^{high}; and CCs were CD77⁻ and CD38^{high} (determined by fluorescence-activated cell sorter [FACS] analysis). Antibodies used for FACS analysis were: anti-IgD-FITC, CD27-FITC, CD38-PE (BD Pharmingen, San Diego, CA), and anti-CD77 plus anti-MURM-FITC (Immunotech, Warrenale, PA).

Microarray expression analysis in primary cells

To analyze *MTA3* and *BCL6* gene expression in normal B-cell subpopulations, we used primary expression data from the purified naive CBs, CCs, and memory B cells.¹⁸ The dataset was filtered to select the genes that meet threshold and variation index criteria,¹⁹ and expression of *MTA3* (223311 s at) and *BCL6* (203140 s at; Affymetrix probe set; Affymetrix, Santa Clara, CA) was analyzed and visualized as a heat map using dChip 2006 software (Dana Farber Cancer Institute, Boston, MA).

Microarray expression analysis in human DLBCLs

MTA3 and *BCL6* expression in primary DLBCLs of the BCR, OxPhos (oxidative phosphorylation), and host response (HR) subtypes as well as the GCB, activated B-cell (ABC), and type 3 subtypes were assessed using a previously published dataset.²⁰ Since the signature of HR tumors is largely defined by normal tumor-infiltrating host inflammatory and immune cells, the analysis was focused on BCR and OxPhos DLBCLs. Expression of

MTA3 and *BCL6* was assessed using signals extracted from representative probe sets (223311 s at, 203140 s at, and 235668 at, respectively, Affymetrix) and visualized using the dChip 2006 software. Statistical analyses were performed with Statistica 6.0 program (Statsoft, Tulsa, OK). The Mann-Whitney *U* test was used for categorical data, and the Spearman rank correlation was used for continuous variables.

Real-time PCR

RNA was prepared from cells using TRIzol (Invitrogen, Carlsbad, CA). cDNA was prepared using Superscript III First Strand cDNA synthesis kit (Invitrogen) and detected by SyberGreen (Applied Biosystems, Foster City, CA) on an Opticon2 thermal cycler (MJ Research, Waltham, MA). We normalized gene expression to *GAPDH* and expressed values relative to control using the $\Delta\Delta CT$ method. For quantitative polymerase chain reaction (QPCR) primers, see Table S1, available on the *Blood* website (see the Supplemental Tables link at the top of the online article).

siRNA gene knockdown

Two *MTA3*-specific siRNAs and 1 control nontargeting siRNA (Table S1) were purchased from Dharmacon (Lafayette, CO). siRNA (500 nm) was suspended in 100 μ L of solution "T" and introduced into cells using the Amaxa nucleofection G16 program (Amaxa Biosystems, Cologne, Germany).

ChIP

Triplicate ChIP on chip was performed as previously described⁸ in Ramos cells using the above-mentioned BCL6 and actin antibodies. Enrichment of the known *BCL6* target gene *CCL3* was validated before and after ligation-mediated PCR amplification of genomic fragments, which were then labeled and cohybridized with their respective input samples to a custom genomic array representing the genomic loci of *PRDM1* and *CD20* with overlapping 50-mer oligonucleotides (Nimblegen Systems, Madison, WI). For array design and raw results, see Table S2. Specific BCL6 binding to genomic regions was detected by determining the fold enrichment of a 5-oligonucleotide sliding window over input. Novel binding sites for BCL6 and MTA3 were confirmed by quantitative real-time PCR single-locus ChIP (QChIP) as previously described.⁸ For primers, see Table S1.

Tissue microarray

Paraffin tissue was obtained from the Department of Pathology, New York Presbyterian Hospital, after necessary informed consent or exemption was obtained in accordance with Helsinki protocols. The cases were fully anonymized, according to Columbia University and federal provisions. All lesions were classified in accordance with the World Health Organization (WHO) classification system. Tissue microarrays were generated using a Beecher Instruments microarrayer (Silver Spring, MD) as previously published.²¹

Immunohistochemistry

Immunostaining with PRDM1 and other antibodies was done essentially as previously published.²²⁻²⁴ The full list of antibodies are listed in Table S3. Briefly, deparaffinized slides were antigen-retrieved in 1 mM EDTA (pH 8); then, a first single indirect immunohistochemistry was performed with either alkaline phosphatase (AP) or biotinylated secondary antibodies, followed by avidin-horseradish peroxidase (HRP) and NBT/BCIP or AEC color development, respectively. Thereafter, the slides were briefly boiled in 1 mM EDTA antigen retrieval solution (pH 8), a second indirect immunohistochemistry (IHC) stain was applied with noncrossreacting reagent, and the slides were finally developed with a contrasting color. For PRDM1 antibody, sections were first antigen-retrieved, cooled, incubated for 30 minutes with deoxyribonuclease I (Sigma) at 5 U/mL in TBS (pH 7.5), blocked with 10% eggwhite (All White; Papetti Foods, Elizabeth, NJ) in PBS for 30 minutes, washed in TBS-Triton X100 (TBS-T), then blocked for 30 minutes with 5% defatted powdered milk in TBS-T and, after several washes in TBS-T, incubated overnight with 1:50 dilution of the antibody in TBS-BSA-Na₃. After 2 washes in TBS-T for 15 minutes each, sections

were incubated with rat antimouse IgG1-AP for 45 minutes, washed for 60 minutes in 0.5 M NaCl and 0.005 M TBS, and developed in NBT-BCIP (Roche, Indianapolis, IN) for up to 24 hours. Single staining for immunoglobulin light chains κ and λ was performed using Envision⁺ staining kit (DakoCytomation, Carpinteria, CA) with antigen retrieval as described. Slides were independently analyzed in a blinded fashion by 2 pathologists and scored as previously published.²⁵

Image acquisition and analysis

Images were taken using a Nikon E600 microscope (Nikon USA, Melville, NY) fitted with Planachromat 4 \times /0.10, 10 \times /0.25, 20 \times /0.40 or PlanApo 40 \times /0.95 objectives for light microscopy; or PlanFluor 10 \times /0.30, 40 \times /0.75 or 60 \times /0.80 objectives for immunofluorescence and SPOT-2 CCD camera and software (Diagnostic Instruments, Sterling Heights, MI). Images were analyzed and assembled with Adobe Photoshop 7 and Adobe Illustrator (Adobe Systems, San Jose, CA).

Cell viability

A total of 2 \times 10⁶ SUDHL4 cells in 2 mL media were treated with 10 μ M BPI, 10 μ g MTA3 siRNA (electroporated), MTA3 siRNA plus BPI, and appropriate controls (negative control peptide and siControl siRNA) in 6-well plates. After 48 hours, 100 μ L cells were plated in 96-well plates (8 replicates per condition), and 20 μ L CellTitre Blue Reagent (Promega, WI) was added per well. After 1 hour, fluorescence was measured at 590 nm in an enzyme-linked immunosorbent assay (ELISA) plate reader. Cell viability was measured using a standard curve prepared similarly.

Results

MTA3 and BCL6 proteins are coexpressed in primary human centroblasts

Although MTA3 and BCL6 were reported to be coexpressed in reactive lymph nodes,¹⁷ these are heterogeneous structures. We wished to specifically define the normal distribution of MTA3 in lymphoid populations and the extent of its endogenous coexpression with BCL6. We first performed MTA3 (blue)/CD20 (brown) immunohistochemistry in human tonsillar reactive lymphoid follicles, in which MTA3 expression appeared limited to CD20⁺ B cells (Figure 1A). More specifically, MTA3 was expressed in the nuclei of GC B cells and was most abundant in the highly proliferative GC dark-zone centroblasts, a BCL6-dependent cell type (Figure 1A).^{3,4,16} Dual-color immunofluorescence confirmed that BCL6 and MTA3 were coexpressed in the same GC cells (Figure 1B). Closer examination of GC cells shows that MTA3 (red) and BCL6 (green) overlap in most B cells, as indicated by the varying degrees of yellow signal, although a few cells seem to preferentially express one or the other (circles in Figure 1B). Moreover, MTA3 was not present in more differentiated B cells, T cells, or histiocyte cells, as shown in costaining experiments with CD138, CD3, and CD68 antibodies, respectively (Figure 1C). To verify that MTA3 and BCL6 are coexpressed in GC B cells, we purified CBs and NBCs from human tonsils and measured the respective mRNA and protein levels (Figure 1D,E). MTA3 and BCL6 were expressed in CBs but not in NBCs (Figure 1D,E). Analysis of an expression microarray dataset from tonsillar B-cell populations confirmed and extended these results, revealing coordinate expression of *BCL6* and *MTA3* in GC CBs and CCs but not pre (naive)– or post (memory)–GC B cells (Figure 1F). Taken together, these studies define the physiologic compartment of MTA3 expression in active lymphoid tissue and demonstrate its coexpression with BCL6 within GC B cells.

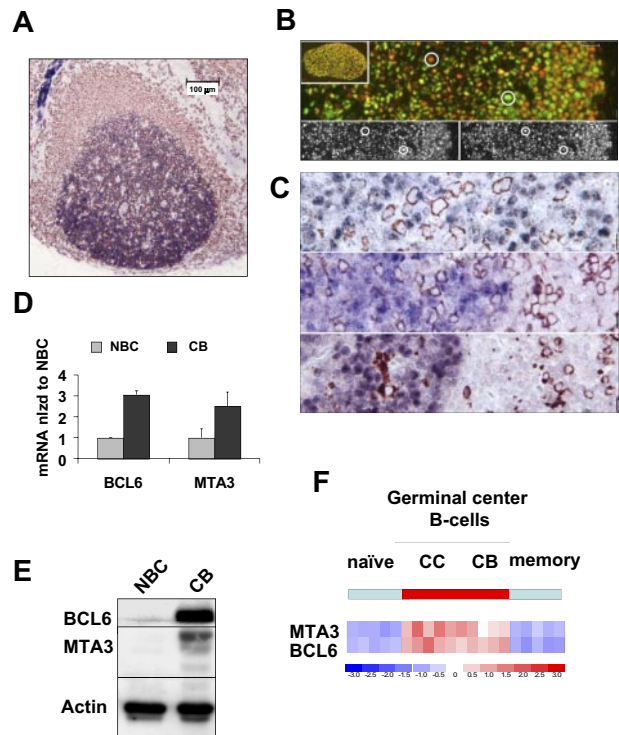


Figure 1. MTA3 is coexpressed with BCL6 exclusively within GC B cells. (A-C) Immunohistochemistry in lymphoid follicle with GC from human tonsil. A CD20 (brown) and MTA3 (blue). (B) Dual immunofluorescence in which MTA3 is labeled in red and BCL6 in green. Cells expressing both proteins display a yellow signal. The circles denote cells used as a reference in the lower 2 panels to demonstrate lack of bleed-through between the fluorescence channels. (C) MTA3 (blue in all 3 panels) along with either CD138 (plasma cell marker), CD3 (T-cell marker), and CD68 (histiocyte marker) respectively, all in brown. (D-F) Purified human tonsillar NBCs and CBs were assessed by (D) real-time PCR for BCL6 and MTA3 mRNA (where the y-axis depicts mRNA abundance normalized to the level found in NBCs). Error bars are SD. (E) Immunoblots with antibodies for MTA3, BCL6, and actin as loading control. (F) Expression microarray analysis visually represented here by a heat map of mRNA levels in NBCs, CCs, CBs, and memory B cells. The scale shows relative mRNA abundance (red = higher, blue = lower).

MTA3 and BCL6 are coordinately expressed in DLBCL

We next asked whether *BCL6* and *MTA3* were coordinately regulated in primary DLBCLs. The expression profiles of 176 patients with DLBCL were explored for mRNA abundance of *BCL6* and *MTA3* (Figure 2A). This analysis revealed that the *MTA3* and *BCL6* mRNA expression is significantly correlated in DLBCL ($R = 0.57$; $P < .001$; Figure 2B). DLBCLs have been classified on the basis of gene expression signature similarities to normal B-cell subsets: GCB, ABC, and an undefined group (type 3)^{26,27}; or, on the basis of reproducible gene signature differences between tumors as determined by comprehensive clustering (BCR, OxPhos, and HR).²⁰ Median *MTA3* expression was higher in the GCB category ($P < .001$) of the former or in the BCR category ($P < .001$) of the latter classification scheme by Mann-Whitney U test. However, expression of *MTA3* and *BCL6* was highly correlated in all patients regardless of their subgrouping, indicating that expression of these genes is tightly linked from the biological standpoint.

To determine whether similar correlation occurred at the protein level, we examined the tumor biopsies from 74 patients with DLBCL by immunohistochemical analysis for MTA3 and BCL6 (Figure 2C). The number of cells (frequency) and intensity of staining were graded by 2 independent pathologists, and the

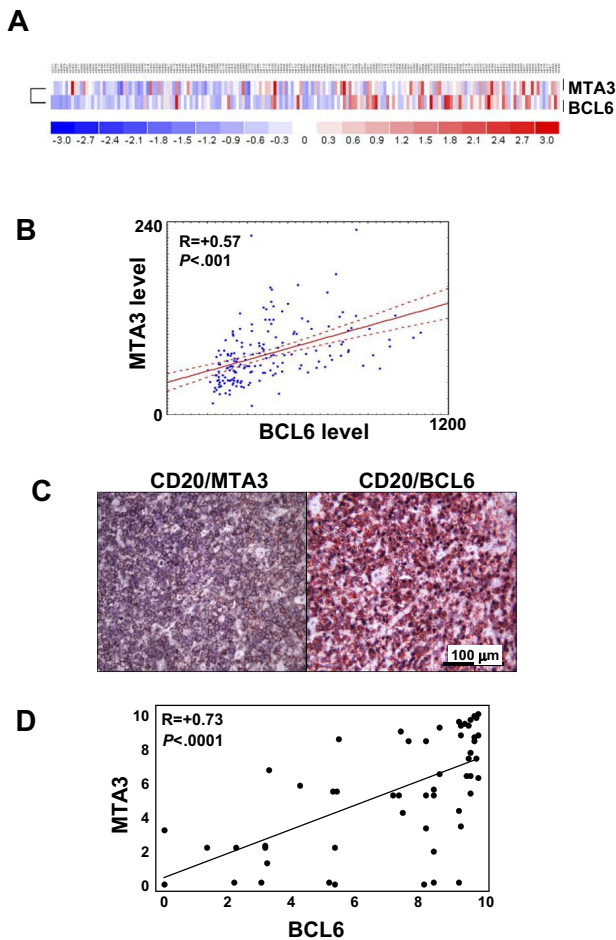


Figure 2. MTA3 and BCL6 expression are highly correlated in primary DLBCLs. (A) BCL6 and MTA3 expression was examined in a panel of 176 patients with DLBCL by expression microarray analysis. A heat map graphically representing BCL6 and MTA3 mRNA abundance is shown. (B) Scatterplot representation of correlation between BCL6 and MTA3 mRNA levels in all patients with DLBCL. The y- and x-axes correspond to mRNA levels in arbitrary units. The lines are regression line with confidence intervals ("Microarray expression analysis in human DLBCLs"). (C) Immunohistochemistry was performed in tissue microarrays (TMAs) containing 74 patients with DLBCL with BCL6, MTA3, and CD20 antibodies. Representative micrographs are shown of a DLBCL sample stained for BCL6 + CD20 or MTA3 + CD20 as labeled. (D) Scatterplot representation of correlation between BCL6 and MTA3 protein levels in all 127 patients with DLBCL. The y- and x-axes represent protein expression levels.

numeric values were compared using the Pearson rank correlation. Of these patients, 54 (72.9%) scored positive for BCL6 and 53 (71.6%) scored positive for MTA3; there was a statistically significant linear correlation ($R = 0.73$; $P < .001$) between the protein levels of MTA3 and BCL6 in these tumors (Figure 2D). These results indicate that MTA3 is coexpressed with BCL6 in DLBCL and therefore might contribute to its lymphomagenic effects.

MTA3 mediates differentiation blockade in DLBCL cells

To study the biological effects of MTA3, we first verified its presence by Western blotting in the 2 BCL6⁺ DLBCL cell lines Ly1 and SUDHL4⁸ (Figure 3A). Exposure to BPI rapidly induces expression of BCL6 target genes involved in survival and proliferation in these cells, including *ATR* and *TP53*, which indicates that BCL6-mediated repression of these genes are dependent on the N-CoR and SMRT corepressors.^{5,8,16,28} However, BPI does not induce differentiation-related BCL6 target genes like *PRDM1*.¹⁶

To determine whether PRDM1 and differentiation was dependent on MTA3 in DLBCL cells, we transfected Ly1 cells with 2 different MTA3 siRNA duplexes or a scrambled negative control. MTA3 depletion was achieved in more than 95% of cells. In contrast to BPI, MTA3 depletion induced PRDM1 mRNA, as well as the plasma cell marker syndecan (the latter presumably as a secondary effect since syndecan is not a BCL6 target gene), but had no effect on *ATR* or *TP53* (Figures 3B, S1). Depletion of MTA3 and induction of PRDM1 by siRNA was confirmed by immunoblotting and densitometry (Figures 3C,D and S1). In accordance with these results, MTA3 expression was mutually exclusive with PRDM1 in human tonsillar germinal centers (Figure 3E; low-power [$\times 10$] view in inset). Finally, depletion of MTA3 induced phenotypic plasma cell differentiation in Ly1 cells, as shown by immunohistochemistry for PRDM1 and intracytoplasmic light chains (Figures 3F, S1). Similar results were obtained in SUDHL4 cells (Figure S2). These results suggest that BCL6 might be able to recruit MTA3 to the *PRDM1* locus (and possibly other differentiation-related loci) to mediate differentiation blockade in DLBCL cells.

BCL6 and MTA3 form a complex on the PRDM1 locus

We next mapped the *PRDM1* locus to identify the site(s) of endogenous BCL6 binding. Although a previous study mapped a BCL6 binding site in *PRDM1* intron 5 in a lymphoblastoid cell line engineered to overexpress BCL6,¹⁰ endogenous binding of *PRDM1* by BCL6 has not been shown. In previous reporter assays, BCL6 was shown to act as a corepressor for AP-1, which binds to the *PRDM1* promoter.¹¹

We performed BCL6 ChIP-on-chip assay using a custom tiling array spanning from approximately 5000 bp upstream of the *PRDM1* transcriptional start site to approximately 3000 bp downstream of its stop codon. The array consisted of 50-mer oligonucleotides with 25-bp overlap in which repeat-masking was used to avoid repetitive elements. The *GAPDH* locus was represented in a similar manner as a negative control. ChIP on chip was performed in triplicate in Ramos B-cell lymphoma cells (a robust cell line for ChIP-on-chip studies⁸) using BCL6 or actin (negative control) antibodies. In all 3 replicates, BCL6 (but not actin antibodies) strongly enriched a set of 23 probes covering approximately 600 bp within *PRDM1* intron 3 (Figure 4A; Table S1). This region corresponds to chr6:106,652,023–106,652,639 and contains at least 1 canonical BCL6 binding site (Figure 4A). In contrast, BCL6 did not bind the *GAPDH* locus (Table S1). To determine whether BCL6 and MTA3 could form a complex at this site, single-locus QChIP was performed in triplicate in both Ramos and Ly1 cells using antibodies for both proteins and primers surrounding the *PRDM1* intron 3 BCL6 binding site. MTA3 and BCL6 were both present at this site but not on the *CD20* promoter, which was used as a negative control (Figure 4B,C). MTA3 binding was dependent on BCL6 since MTA3 could not bind to *PRDM1* in Mutu III B cells, which express MTA3 but not BCL6 (Figure 4D). Taken together, these data show that in DLBCL cells, BCL6 represses *PRDM1* through an intron 3 binding site and blocks differentiation through recruitment of MTA3: as previously reported, BCL6 also mediates growth and survival preferentially through SMRT binding to *TP53* and other genes such as *ATR*.^{5,6,28}

MTA3 depletion does not kill DLBCL cells alone, but can enhance the antilymphoma effects of BPI

Targeting transcription factors has been shown to be an effective therapeutic strategy for several cancers.²⁹ To determine whether MTA3 targeting has antilymphoma effects, we measured cell

Figure 3. MTA3 depletion is associated with differentiation of DLBCL cells. (A) MTA3 Immunoblots were performed in LY1 and SUDHL4 DLBCL cell lines—actin is shown as loading control. (B) Immunoblots for MTA3, PRDM1, and actin performed in Ly1 cells (left) and SUDHL4 cells (right) transfected with MTA3 siRNA or ctrl siRNA. (C) MTA3 siRNA knockdown was performed in Ly1 (left panel) and SUDHL4 cells (right panel), followed in 24 hours by QPCR for the *MTA3*, *PRDM1*, *SDC1*, *TP53*, and *ATR* transcripts. The y-axis represents the fold change in mRNA abundance relative to the levels in wild-type and control siRNA-transfected cells. Error bars are SD. (D) Dual immunofluorescence of a human tonsillar GC with MTA3 (red) and PRDM1 (green) antibodies. The inset is the same GC at low-power magnification. (E) Ly1 cells were transfected with MTA3 or control siRNA and examined by immunohistochemistry for expression of MTA3, PRDM1, and κ light chains with corresponding antibodies.

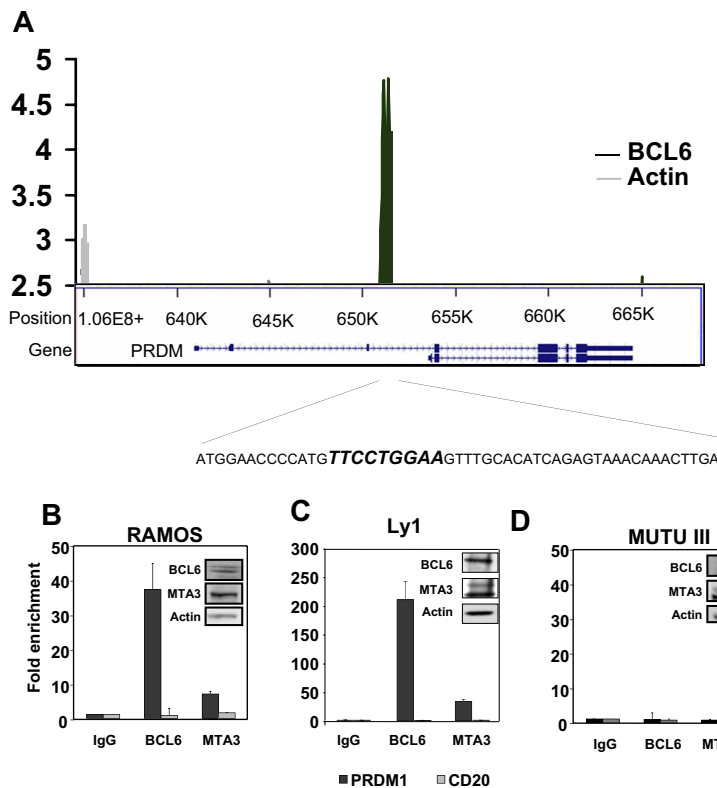
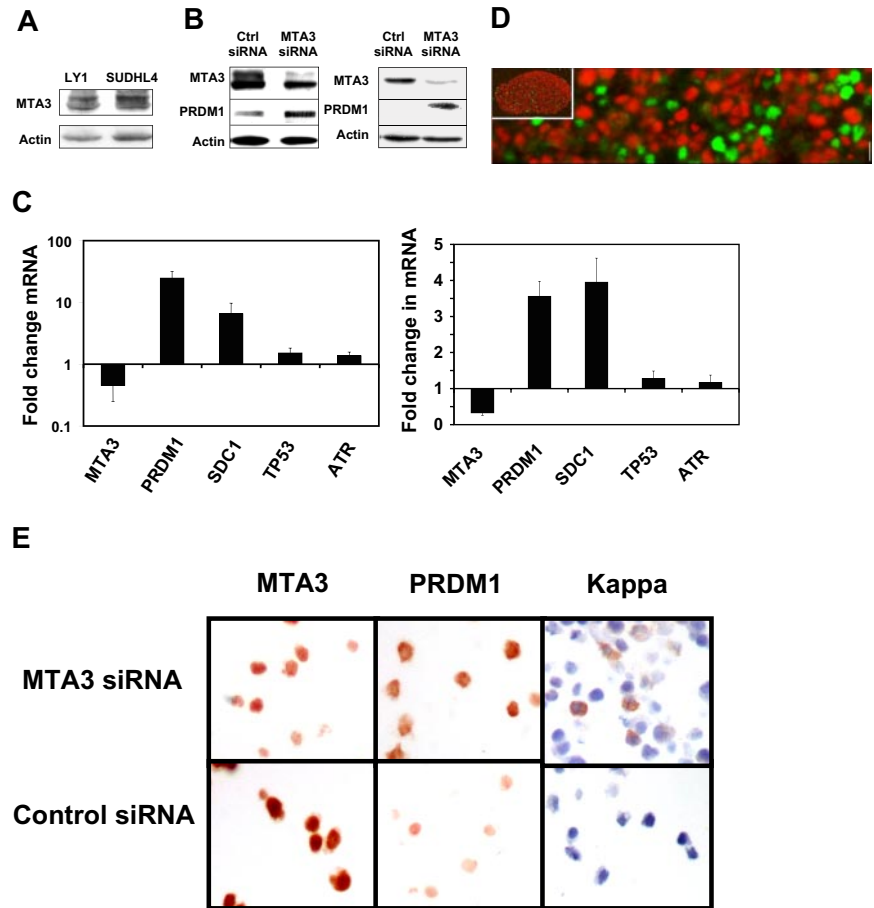


Figure 4. BCL6 recruits MTA3 to a binding site located within intron 3 of the human *PRDM1* locus. (A) Graphic representation of tiling ChIP on chip performed on the *PRDM1* genomic locus in Ramos cells. The top portion of the graph shows fold enrichment of sequences within intron 3 by BCL6 (■) or actin (□) antibodies versus input. The corresponding graphic representation of the *PRDM1* locus (bottom) indicates the location of BCL6 binding, and the amplicon containing the BCL6 binding site that was used for QChIP in panels B-D. (B) QChIP was performed with BCL6, MTA3, and actin antibodies in Ramos cells for the site shown in panel A as well as a negative control promoter (CD20). The y-axis represents fold enrichment of the site relative to control (actin) antibody. Inset shows immunoblot of BCL6, MTA3, and actin in Ramos B-cell lymphoma cells. (C-D) Similar QChIP was performed in Ly1 DLBCL cells and in the BCL6⁻Mutu III B-cell lymphoma cells, respectively. Error bars are SD.

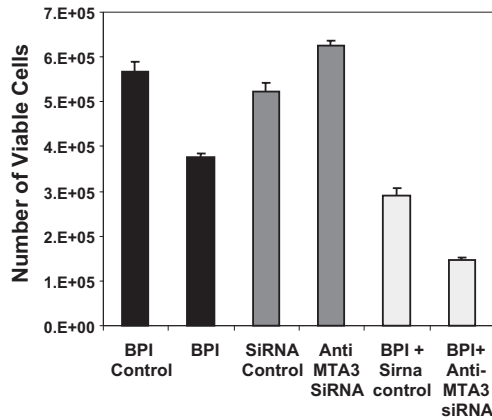


Figure 5. MTA3 depletion alone does not kill lymphoma cells but synergizes in combination with BPI. SUDHL4 DLBCL cells were exposed to BPI, control peptide, MTA3 siRNA, or control siRNA alone or in combination, and the cell viability was measured by reduction of resazurin 48 hours after the beginning of the experiment (performed in 8 replicates). The y-axis corresponds to the number of viable cells at 48 hours. Error bars are SD.

viability in DLBCL cells after siRNA depletion. In these experiments we used SUDHL4 cells, which are highly BCL6 dependent and most sensitive to BCL6 blockade by BPI.⁸ MTA3 depletion had no effect on viability in these cells (Figure 5) or Ly1 cells (not shown). This result is in contrast with BPI, which mediates cell death and cell-cycle arrest, but has no effect on differentiation (Polo et al¹⁶; Figure 5). Although MTA3 knockdown alone did not kill lymphoma cells, we asked whether blocking the functions of both the BCL6 BTB domain (with BPI) and the BCL6 RD2 (by depleting MTA3) enhanced antilymphoma effects. The combination of MTA3 depletion plus BPI had a synergistic antilymphoma effect (Figures 5, S1), suggesting that more complete inhibition of BCL6, hitting 2 rather than 1 of its biochemical functions, could be a more potent form of antilymphoma therapy for DLBCL.

Discussion

This report shows that BCL6 uses 2 sets of corepressors to repress genes involved in 2 distinct biologic pathways. Whereas SMRT/N-CoR corepressor binding to the lateral groove motif of the BCL6 BTB domain modulates survival, MTA3 binding to its second repression domain blocks cellular differentiation (Figure 6). The former effects are mediated mainly by repression of genes such as *ATR* and *TP53*, while the latter involves repression of *PRDM1*. This result was surprising to us, since the prevailing view is that within a given cell, transcription factors like BCL6 recruit a constellation of cofactors that are collectively required to exert full silencing of their different target genes. There is a rationale for transcriptional regulation to be organized in such a manner, since by signaling to certain corepressors, B cells could modulate specific BCL6-dependent pathways while leaving others intact—thus allowing finer tuning of the cellular phenotype. In accordance with this scenario, we have shown that CD40 signaling can rapidly disrupt the interaction of BCL6 with SMRT and N-CoR, but has no effect on MTA3⁵ so that BCL6 can no longer protect cells from DNA damage but still blocks differentiation.

BCL6 interacts with multiple other corepressors, which raises the possibility that additional pathways might be regulated through still more biochemical mechanisms. For example, BCL6 also interacts with the ETO corepressor through its C-terminal zinc

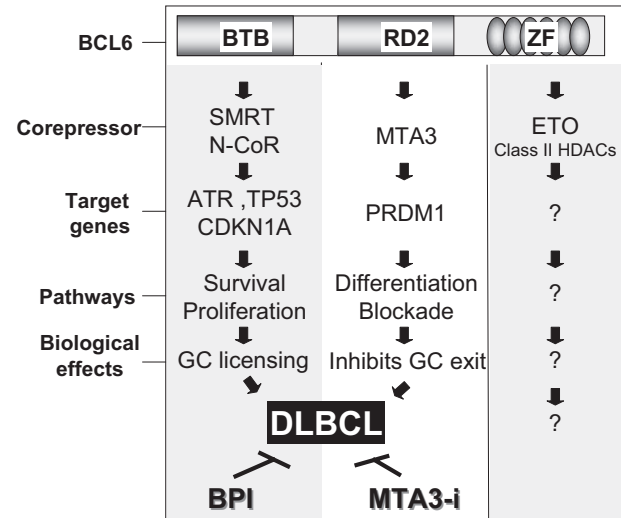


Figure 6. BCL6 mediates lymphomagenesis through 2 distinct pathways. Our data suggest a model where recruitment of SMRT, N-CoR, and BCoR through the BCL6 BTB domain mediates repression of *ATR*, *TP53*, and *CDKN1A*, which facilitates survival and proliferation. This allows activated B cells to acquire the CB phenotype and is required for survival of DLBCL. On the other hand, recruitment of the MTA3 protein through the RD2 mediates repression of *PRDM1* and hence blocks differentiation, preventing B cells from exiting the GC and contributing to lymphomagenesis. The ETO corepressor and class II HDACs bind to the zinc finger region of BCL6, but their functions are unknown. Combined blockade of the BTB and RD2 biochemical mechanisms of action of BCL6 results in more profound disruption of the BCL6 oncogenic transcriptional program and enhanced DLBCL cell death.

fingers³⁰ (Figure 6). ETO was shown to enhance repressor activity of BCL6 and to form a complex with BCL6 on the cyclin D2 promoter.³⁰ The biological impact of ETO on BCL6 function is not yet known, but might reveal additional complexity in the BCL6 transcriptional program. There is room for such complexity, since the BCL6 transcriptional program includes more pathways than survival and differentiation. Our ChIP-on-chip genomic localization studies indicated that BCL6 could bind to approximately 500 targets, corresponding to genes involved in protein ubiquitylation, metabolism, cell cycle, DNA damage response, chromatin modifications, and others.⁸ Moreover, BCL6 interacts with a number of additional cofactors,³¹ suggesting that further functional diversification could exist. The current results suggest that these pathways can be functionally compartmentalized and manipulated for therapeutic benefit in DLBCLs.

PRDM1 is a critical target gene of BCL6 in GC differentiation since it is a master regulator required for B cells to adopt the plasma cell phenotype.¹² Regulation of *PRDM1* by BCL6 was first suggested by microarray studies in cells expressing dominant-negative BCL6 constructs.⁹ Both direct and indirect BCL6 regulation of *PRDM1* have since been described.^{10,11} Fujita et al showed that *PRDM1* levels (1) increased upon depletion of MTA3 in Burkitt lymphoma cells and (2) decreased in myeloma cells in which MTA3 and BCL6 were ectopically expressed.¹⁷ In order to study the action of BCL6 on *PRDM1*, we rigorously mapped the *PRDM1* locus for BCL6 binding. We chose ChIP-on-chip, since it allows in vivo binding to be detected in cells with endogenous BCL6. In these experiments, we did not observe binding at the intron 5 element reported by Tunaypin et al.¹⁰ In the report by Tunaypin et al, BCL6 was ectopically expressed in WI-L2 lymphoblastoid cells, in contrast to the current experiments with endogenous BCL6 in lymphoma cells. It is possible that the intron 5 binding was due to BCL6 overexpression, or was specific to lymphoblastoid cells but not lymphoma cells. We also did not see

binding of BCL6 in the *PRDM1* promoter region near AP-1 binding sites as suggested by Vasawala et al.¹¹ Reasons for this difference could be that BCL6 does not bind to the *PRDM1* promoter through AP1 in the Ramos or Ly1 lymphoma cells used in this study. Alternatively, indirect binding of BCL6 may not be captured by ChIP assays, which occasionally occurs in the case of certain cofactors that associated with genes through other factors (such as the case of BCL6 when it interacts with AP-1). In contrast, we found that endogenous BCL6 powerfully enriched a 600-bp region in intron 3; 23 consecutive probes were reproducibly and specifically enriched. Moreover, we showed that MTA3 binds to this site in a BCL6-dependent manner, suggestive of a BCL6-dependent repression complex. MTA3 ChIP enrichment of the *PRDM1* locus was less than that of BCL6. This is a common finding in ChIP assays because corepressor antibodies, which associate indirectly with DNA, are less efficient at enriching chromatin fragments than DNA-binding transcription factor antibodies.

Consistent with the importance of its partnership with BCL6, MTA3 expression was found exclusively within the CBs and CCs of the GC, and not in any other cell type present within lymphoid follicles. Moreover, MTA3 and BCL6 expression was tightly correlated in primary DLBCLs, many of which presumably arise from GC cells. Taken together with the rest of the data, our results suggest that BCL6 mediates differentiation blockade in DLBCL by recruiting MTA3 to the intron 3 of *PRDM1*. Differentiation therapy using all-*trans* retinoic acid (ATRA) in acute promyelocytic leukemia (APL) ameliorates the leukemic phenotype without causing apoptosis;³² this approach has proven to be successful in patients.³³ From a therapeutic standpoint, MTA3 depletion caused differentiation but did not kill cells *in vitro*, but similar to the ATRA/APL paradigm, it is possible that differentiation might still be an effective therapeutic goal in DLBCL. Our combination studies using both BPI and MTA3 depletion more effectively inhibited lymphoma cell viability than either modality alone. These data highlight the importance of targeting several functional domains to maximally inhibit transcription factors involved in oncogenesis. We propose that the targeting of MTA3/BCL6

interaction with peptide or small molecules in combination with BPI might be useful in this context.

Taken together, we conclude that BCL6 mediates differentiation blockade in DLBCLs via its interaction with MTA3: this supports a model of lymphomagenesis where BCL6 controls the cell survival program via the interaction of its BTB domain with SMRT and simultaneously causes differentiation blockade via the interaction of the RD2 domain with MTA3 (Figure 6). Combination therapy for both pathways controlled by BCL6 in DLBCL pathogenesis is possible by targeting dual repression domain function simultaneously.

Acknowledgments

We thank the Histopathology Shared Resource of the Albert Einstein Cancer Center for their invaluable assistance. We apologize to the many investigators whose work could not be discussed due to space limitations.

S.P. is a recipient of the American Society of Clinical Oncology Young Investigator Award. A.M.M. is supported by National Cancer Institute grant no. R01 CA104348, the Leukemia and Lymphoma Society, Chemotherapy Foundation, Samuel Waxman Cancer Research Foundation, and the G&P Foundation.

Authorship

Contribution: S.P., J.M.P., and P.J. designed and performed the research, analyzed data, and wrote the paper. P.L., Y.Y., U.K., and S.M.R. designed and performed the research and analyzed data. R.S. and G.C. designed and performed the research, analyzed data, and wrote the paper. R.D.F., M.S., and A.M.M. designed the research, analyzed data, and wrote the paper.

Conflict-of-interest disclosure: The authors declare no competing financial interests.

Correspondence: Ari Melnick, Albert Einstein College of Medicine, Chanin 302A, Bronx, NY 10461; e-mail: amelnick@aecom.yu.edu.

References

- Ye BH, Lista F, Lo Coco F, et al. Alterations of a zinc finger-encoding gene, BCL-6, in diffuse large-cell lymphoma. *Science*. 1993;262:747-750.
- Wang X, Li Z, Naganuma A, Ye BH. Negative autoregulation of BCL-6 is bypassed by genetic alterations in diffuse large B cell lymphomas. *Proc Natl Acad Sci U S A*. 2002;99:15018-15023.
- Dent AL, Shaffer AL, Yu X, Allman D, Staudt LM. Control of inflammation, cytokine expression, and germinal center formation by BCL-6. *Science*. 1997;276:589-592.
- Ye BH, Cattoretti G, Shen Q, et al. The BCL-6 proto-oncogene controls germinal-center formation and Th2-type inflammation. *Nat Genet*. 1997;16:161-170.
- Ranuncolo SM, Polo JM, Dierov J, et al. Bcl-6 mediates the germinal center B cell phenotype and lymphomagenesis through transcriptional repression of the DNA-damage sensor ATR. *Nat Immunol*. 2007;8:705-714.
- Phan RT, Dalla-Favera R. The BCL6 proto-oncogene suppresses p53 expression in germinal-center B cells. *Nature*. 2004;432:635-639.
- Phan RT, Saito M, Basso K, Niu H, Dalla-Favera R. BCL6 interacts with the transcription factor Miz-1 to suppress the cyclin-dependent kinase inhibitor p21 and cell cycle arrest in germinal center B cells. *Nat Immunol*. 2005;6:1054-1060.
- Polo J, Juszczynski P, Monti S, et al. A transcriptional signature with differential expression of BCL6 target genes identifies BCL6-dependent diffuse large B-cell lymphomas. *Proc Natl Acad Sci U S A*. 2007;104:3207-3212.
- Shaffer AL, Yu X, He Y, Boldrick J, Chan EP, Staudt LM. BCL-6 represses genes that function in lymphocyte differentiation, inflammation, and cell cycle control. *Immunity*. 2000;13:199-212.
- Tunayapin C, Shaffer AL, Angelin-Duclos CD, Yu X, Staudt LM, Calame KL. Direct repression of *prdm1* by Bcl-6 inhibits plasmacytic differentiation. *J Immunol*. 2004;173:1158-1165.
- Vasawala FH, Kusam S, Toney LM, Dent AL. Repression of AP-1 function: a mechanism for the regulation of Blimp-1 expression and B lymphocyte differentiation by the B cell lymphoma-6 protooncogene. *J Immunol*. 2002;169:1922-1929.
- Lin KI, Tunayapin C, Calame K. Transcriptional regulatory cascades controlling plasma cell differentiation. *Immunol Rev*. 2003;194:19-28.
- Huynh KD, Bardwell VJ. The BCL-6 POZ domain and other POZ domains interact with the corepressors N-CoR and SMRT. *Oncogene*. 1998;17:2473-2484.
- Huynh KD, Fischle W, Verdin E, Bardwell VJ. BCoR, a novel corepressor involved in BCL-6 repression. *Genes Dev*. 2000;14:1810-1823.
- Ahmad KF, Melnick A, Lax S, et al. Mechanism of SMRT corepressor recruitment by the BCL6 BTB domain. *Mol Cell*. 2003;12:1551-1564.
- Polo JM, Dell'Oso T, Ranuncolo SM, et al. Specific peptide interference reveals BCL6 transcriptional and oncogenic mechanisms in B-cell lymphoma cells. *Nat Med*. 2004;10:1329-1335.
- Fujita N, Jaye DL, Geigerman C, et al. MTA3 and Mi-2/NuRD complex regulate cell fate during B-lymphocyte differentiation. *Cell*. 2004;119:75-86.
- Klein U, Tu Y, Stolovitzky GA, et al. Transcriptional analysis of the B cell germinal center reaction. *Proc Natl Acad Sci U S A*. 2003;100:2639-2644.
- Juszczynski P, Kutok JL, Li C, Mitra J, Aguiar RC, Shipp MA. BAL1 and BBAP are regulated by a gamma interferon-responsive bidirectional promoter and are overexpressed in diffuse large B-cell lymphomas with a prominent inflammatory infiltrate. *Mol Cell Biol*. 2006;26:5348-5359.
- Monti S, Savage KJ, Kutok JL, et al. Molecular profiling of diffuse large B-cell lymphoma identifies robust subtypes including one characterized by host inflammatory response. *Blood*. 2005;105:1851-1861.

21. Shaknovich R, Celestine A, Yang L, Cattoretti G. Novel relational database for tissue microarray analysis. *Arch Pathol Lab Med*. 2003;127:492-494.
22. Cattoretti G, Chang CC, Cechova K, et al. BCL-6 protein is expressed in germinal-center B cells. *Blood*. 1995;86:45-53.
23. Chang DH, Cattoretti G, Calame KL. The dynamic expression pattern of B lymphocyte induced maturation protein-1 (Blimp-1) during mouse embryonic development. *Mech Dev*. 2002;117:305-309.
24. Houldsworth J, Olshen AB, Cattoretti G, et al. Relationship between REL amplification, REL function, and clinical and biologic features in diffuse large B-cell lymphomas. *Blood*. 2004;103:1862-1868.
25. Cattoretti G, Buttner M, Shaknovich R, Kremmer E, Alobeid B, Niedobitek G. Nuclear and cytoplasmic AID in extrafollicular and germinal center B cells. *Blood*. 2006;107:3967-3975.
26. Alizadeh AA, Eisen MB, Davis RE, et al. Distinct types of diffuse large B-cell lymphoma identified by gene expression profiling. *Nature*. 2000;403:503-511.
27. Rosenwald A, Wright G, Chan WC, et al. The use of molecular profiling to predict survival after chemotherapy for diffuse large-B-cell lymphoma. *N Engl J Med*. 2002;346:1937-1947.
28. Cerchiatti L, Polo J, DaSilva G, et al. BCL6, p53 and molecular targeted therapy in B-cell lymphomas. *Blood*. 2005;106: Abstract 1484.
29. Melnick AM, Adelson K, Licht JD. The theoretical basis of transcriptional therapy of cancer: can it be put into practice? *J Clin Oncol*. 2005;23:3957-3970.
30. Chevallier N, Corcoran CM, Lennon C, et al. ETO protein of t(8;21) AML is a corepressor for Bcl-6 B-cell lymphoma oncoprotein. *Blood*. 2004;103:1454-1463.
31. Miles RR, Crockett DK, Lim MS, Elenitoba-Johnson KS. Analysis of BCL6-interacting proteins by tandem mass spectrometry. *Mol Cell Proteomics*. 2005;4:1898-1909.
32. Melnick A, Licht JD. Deconstructing a disease: RARalpha, its fusion partners, and their roles in the pathogenesis of acute promyelocytic leukemia. *Blood*. 1999;93:3167-3215.
33. Tallman MS, Nabhan C, Feusner JH, Rowe JM. Acute promyelocytic leukemia: evolving therapeutic strategies. *Blood*. 2002;99:759-767.